Interdecadal change in the influence of El Niño in the developing stage on the central China summer precipitation

Lin Chen[1] · Gen Li[1,2] · Shang-Min Long[1] · Chujie Gao[1,3] · Zhiyuan Zhang[1,4] · Bo Lu[5]

Abstract

The central China summer precipitation (CCSP) is of great importance to the people's livelihood of this densely populated region, including the agriculture, ecosystems, water resources, economies, and health. Based on the observed precipitation, sea surface temperature (SST), and atmospheric reanalysis datasets, the present study investigates the effects of El Niño in the developing stage on the CCSP during 1960–2014. The results show that the CCSP anomalies exhibit significant negative correlations with the El Niño-related SST anomalies in both the simultaneous summer and the following winter, implying that the developing El Niño is important for modulating the CCSP. However, this climatic teleconnection of El Niño is unstable, with an obvious interdecadal change around the late 1980s. Specifically, the negative correlation is not statistically significant in the previous epoch before the late 1980s (1960–1988), but dramatically strengthens since the late 1980s (the post epoch for 1989–2014). Such an interdecadal change is closely associated with the change of the El Niño-related SST anomaly pattern. Compared to the previous epoch, the central Pacific El Niño occurs more frequently in the post epoch, leading to an interdecadal shift of the maximum warm SST anomalies from the eastern Pacific to the central Pacific. The resultant westward extension of the atmospheric circulation responses induces an anomalous low-level cyclone covering South China in the post epoch. It would prevent the southwest monsoon from delivering the moisture to the north and hence reduce the CCSP. While, in the previous epoch, the anomalous cyclone locates east of South China, exerting insignificant influence on the CCSP. This work highlights a strengthening effect of El Niño on the CCSP since the late 1980s, with great implications for the regional seasonal climate prediction.

Keywords Interdecadal change · El Niño · Central China summer precipitation · Developing stage · East asian summer monsoon · Atmospheric teleconnection

✉ Gen Li
  ligen@hhu.edu.cn

1   College of Oceanography, Hohai University, Nanjing, China

2   Southern Marine Science and Engineering Guangdong Laboratory (Zhuhai), Zhuhai, China

3   State Key Laboratory of Tropical Oceanography, South China Sea Institute of Oceanology, Chinese Academy of Sciences, Guangzhou, China

4   State Key Laboratory of Loess and Quaternary Geology, Institute of Earth Environment, Chinese Academy of Sciences, Xi'an, China

5   Laboratory for Climate Studies and CMA-NJU Joint Laboratory for Climate Prediction Studies, National Climate Center, China Meteorological Administration, Beijing, China

1 Introduction

The central China locates between the middle reaches of the Yangtze River basin and the middle and lower reaches of the Yellow River basin and is an important agricultural and industrial center (Sun et al. 2010; Ren et al. 2013; Ke and Guan 2014; Hu et al. 2020). The local livelihood of millions of people and development of economies are vulnerable to the variations of summer precipitation, especially the droughts and floods brought by extreme precipitation anomalies (Hu et al. 2020). For example, the severe summer drought in Henan Province in 2014 (Wang et al. 2018) and the record-breaking Meiyu event over the Yangtze River basin in 2020 (Liu et al. 2020; Ding et al. 2021; Qiao et al. 2021; Zheng and Wang 2021; Zhou et al. 2021) seriously threatened the local people's living conditions and garnered much public attention. Thus, it is of great significance to

investigate the variations of the central China summer precipitation (CCSP) and the internal mechanisms.

As an integral part of the East Asian summer monsoon (EASM) system, the CCSP is strongly modulated by the intensity and advancement of the EASM (Hu et al. 2017). Abundant water vapor brought by the strong southwest monsoon, against the cold air from the north, often causes a quasi-stationary rainband over East Asia as a result of frontal activity (Chen et al. 2004; Ding and Chan 2005; Ding 2007; Su and Xue 2010; Chiang et al. 2020; Gao et al. 2020a, b). As the EASM migrates northward, when such a quasi-stationary rainband anchors over the central China, the local heavy precipitation occurs frequently (Ding and Chan 2005; Sampe and Xie 2010; Chiang et al. 2020; Gao et al. 2020a, c), bringing huge impacts to the regional society and economy. Undoubtedly, a better understanding of the variations and causes of the EASM is conductive to grasp those of the CCSP.

El Niño-Southern Oscillation (ENSO) is the dominant interannual mode of the coupled ocean-atmosphere system in the tropics, exerting important influences on the EASM via the atmospheric teleconnection (Zhang and Sumi 1999; Wang et al. 2000, 2021; Chen 2002; Deser et al. 2010; Hu et al. 2017, 2020; Li and Lu 2020; Jiang et al. 2021; Liu et al. 2021). El Niño, as the warm phase of ENSO, generally develops in boreal summer and the early autumn, reaches its peak in boreal winter, and decays in the following spring and summer (An and Wang 2001; Tozuka and Yamagata 2003; Lau et al. 2005; Xie et al. 2009). It has different climate effects on the EASM during different phases (Huang and Wu 1989; Wu et al. 2003, 2009; Cao et al. 2019; Yong and Huang 2019). For the El Niño decaying summer, an anomalous anticyclone exists over the Northwest Pacific (NWP). It could enhance the EASM and transport abundant moisture to the mainland, causing excessive precipitation over the Yangtze River basin (Zhang and Sumi 1999; Chang et al. 2000a, b; Wang et al. 2000, 2003, 2013; Xie et al. 2009; Xie and Zhou 2017; Li et al. 2017b, 2021a; Hu et al. 2017, 2019, 2020). In the past two decades, several theories were formed to explain the maintaining of the anomalous NWP anticyclone during the El Niño decaying summer. These theories include the NWP (Wang et al. 2000, 2013; Li et al. 2017b) or the central Pacific (Wang et al. 2013, 2017; Li et al. 2017b) SST forcing as a Rossby wave response, the forcing of the El Niño-related Indian Ocean basin warming as a Kelvin wave response (Yang et al. 2007; Xie et al. 2009, 2010, 2016; Li et al. 2019), and the nonlinear interaction between ENSO and annual cycle (Stuecker et al. 2013, 2015). All these studies advance the understanding of the effect of the decaying El Niño on the EASM.

While a large number of previous studies focused on the influence of El Niño on the East Asian climate in the decaying summer (Chen et al. 2016, 2018; Xie et al. 2016; Hu et al. 2017, 2020; He et al. 2019), the impacts of El Niño in the developing summer on the East Asian climate, however, are relatively less studied. Previous studies (Wu et al. 2009; Wen et al. 2019, 2020) revealed that there is increased precipitation in the southeastern China and decreased precipitation in the northern-central China during the developing summer of El Niño. In particular, while Wu et al. (2009) attributed this to an anomalous cyclone over the NWP and an anomalous anticyclone over the north Indian Ocean, Wen et al. (2019, 2020) recently ascribed this to an anomalous cyclone over the northeastern Asia and an anomalous anticyclone over the NWP. Therefore, further inspections on the effects of the developing El Niño on the East Asian summer climate, especially the CCSP, may be needed.

In particular, since the late 1980s, the El Niño-related SST anomaly pattern experiences an obvious interdecadal change, with more frequent occurrences of the maximum SST anomalies in the central Pacific instead of the eastern Pacific (Table 1; Ashok et al. 2007; Kug et al. 2009; Yeh et al. 2009; Lee and McPhaden 2010; Pascolini-Campbell et al. 2015; Feng et al. 2020; He et al. 2021; Li et al. 2021b). Compared with the eastern Pacific (EP) El Niño, the central Pacific (CP) El Niño causes different anomalous atmospheric circulations and dry/wet distributions worldwide (Ashok et al. 2007; Weng et al. 2007, 2011; Feng et al. 2010; Karori et al. 2013; Chen et al. 2014; Li et al. 2014, 2021c; Cao et al. 2019; Wen et al. 2020). For example, while the atmospheric circulation anomalies over East Asia and the precipitation anomalies in China are very weak in the developing summer of the EP El Niño, there is an anomalous anticyclone around Japan and anomalous cyclones to its north and south in the CP El Niño developing summer (Weng et al. 2007; Yuan and Yang 2012; Yuan et al. 2012; Chen et al. 2019), which might potentially bring droughts to the central China. Given that the regional climate effects between the EP El Niño and the CP El Niño are distinctly different in the developing summer, here we propose a hypothesis that the increased frequency of the CP El Niño events since the late 1980s might cause an interdecadal change in the effects of the developing El Niño on the East Asian summer climate.

Table 1 A list of the El Niño developing years during 1960–1988 and 1989–2014

Period	Year
1960–1988	1963, 1965, 1969, 1972, 1976, **1977**, 1982, **1987**
1989–2014	1991, **1994**, 1997, **2002**, **2004**, **2006**, **2009**

The bold numbers denote the central Pacific (CP) El Niño years

The present study investigates the El Niño's effects on the CCSP during its developing stage. Indeed, our results show that the relationship between the developing El Niño and the CCSP anomalies is unstable, with an interdecadal strengthening since the late 1980s. The analyses reveal that such an interdecadal change is closely associated with the increased occurrences of the CP El Niño events in the past three decades. The present results identify the CP El Niño as an important source of seasonal predictability of the CCSP since the late 1980s. This implies that an improved El Niño prediction will also be vital to improve the seasonal prediction skills of the CCSP.

The rest of this paper is organized as follows. Section 2 describes the datasets and methods used in this study. Section 3 shows an interdecadal change in the relationships between the developing El Niño and the CCSP anomalies. Section 4 analyzes the possible mechanisms for this interdecadal change. Section 5 is a summary with discussion.

2 Datasets and methods

In this study, the observed precipitation data are taken from the Climate Research Unit (CRU) land-based gridded observations at the University of East Anglia with a resolution of $0.5° \times 0.5°$ (Harris et al. 2014). The monthly SST data ($1.0° \times 1.0°$) are derived from the Hadley Centre of the U.K. Met Office (HadISST; Rayner et al. 2006). The monthly data of atmospheric fields, including the zonal and meridional components of wind, precipitation rate, omega and specific humidity, are taken from the National Centers for Environmental Prediction-National Center for Atmospheric Research (NCEP-NCAR) reanalysis with a horizontal

resolution of $2.5° \times 2.5°$ (Kalnay et al. 1996). The present study period is from 1960 to 2014.

This study investigates the El Niño's effects on the CCSP in the developing stage. For convenience, we denote boreal summer [June–July–August] as JJA, autumn [September–October–November] as SON, and the following winter [December–January–February] as DJF. The CCSP index is defined as the JJA precipitation anomalies averaged over the central China ($28° N–38° N, 100° E–118° E$; Fig. 1). The Niño3.4 index is denoted as the regional-averaged SST anomalies in $5° S–5° N, 170° W–120° W$. The El Niño event is identified by the 3-month running mean Niño3.4 index exceeding the threshold of 0.5 °C and persisting for at least 5 months (also see https://origin.cpc.ncep.noaa.gov/products/analysis_monitoring/ensostuff/ONI_v5.php). According to this definition, we select 15 El Niño developing years (Table 1) for composite analyses. In addition, the CP El Niño years are marked out in Table 1, when the difference of the mature winter SST anomalies between the Niño4 region ($5° S–5° N, 160° E–150° W$) and the Niño3 region ($5° S–5° N, 150° W–90° W$) is larger than zero. Indeed, the CP El Niño events appear more frequently than the EP El Niño events since the late 1980s (Table 1). In this study, we also use a two-tailed Student's t test for the significance test of the correlation and composite analyses.

3 Interdecadal change in the relationships between the developing El Niño and the CCSP

Figure 1a shows the correlations of the JJA precipitation anomalies over East Asia with the simultaneous JJA Niño3.4 index during 1960–2014. There are significant negative

Fig. 1 Correlation coefficients of the summer [June–July–August (JJA)] precipitation anomalies with **a** the simultaneous JJA and **b** the following winter [December–January–February (DJF)] Niño3.4 ($5° S–5° N, 170° W–120° W$) indices during 1960–2014. The dots indicate that the correlations are at a significance level of $p < 0.05$. The box area in each panel denotes the region of the central China ($28° N–38° N, 100° E–118° E$). All data are linearly detrended
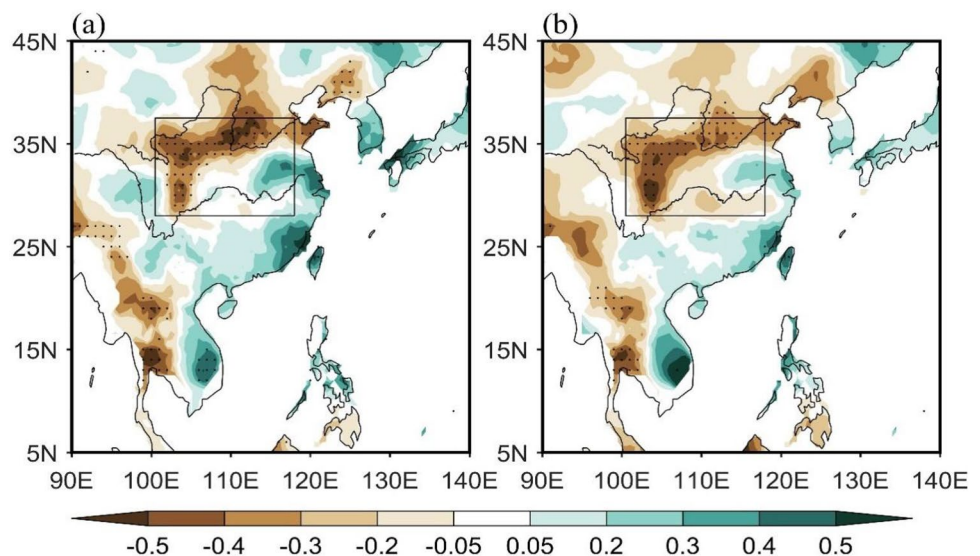
correlations in the central China (28° N–38° N, 100° E–118° E), with large values mainly in the north and west, indicating that the summer precipitation anomalies in the central China are closely associated with the simultaneous SST anomalies in the tropical central and eastern Pacific. As the simultaneous summer correlations cannot well distinguish the El Niño developing stage and decaying stage (Wu et al. 2010), we further present the correlations between the JJA precipitation anomalies and the following DJF Niño3.4 index (Fig. 1b). Obviously, the prominent negative correlations still exist in the central China, similar to that in Fig. 1a. This confirms that the interannual relationship between the developing El Niño and the CCSP anomalies is pronounced.

In Fig. 2a, b, the regressions of the JJA 850-hPa streamfunction and rotational wind anomalies onto the simultaneous JJA and the following DJF Niño3.4 indices are used to explore how the SST anomalies in the tropical central and eastern Pacific affect the precipitation anomalies over the central China. Results show that there is an anomalous

cyclone over South China, which would prevent the southwest monsoon from delivering the moisture to the north, thus resulting in decreased precipitation over the central China. On the one hand, such an anomalous cyclone can be considered as a Gill-type Rossby wave response exerted by the anomalous warming over the central and eastern Pacific (Wang et al. 2013, 2017; Li et al. 2017b). On the other hand, the Walker circulation adjustment can also be considered as a culprit (Weng et al. 2007; Yuan and Yang 2012; Wang et al. 2013; Huang et al. 2018; Li et al. 2017b). Figure 2c, d display the JJA 200-hPa velocity potential and divergent wind anomalies regressed onto the simultaneous JJA and the following DJF Niño3.4 indices, respectively. The upper-level velocity potential and divergent winds are used to reflect the descending and ascending motions of the Walker circulation. Here the negative velocity potential combined with the divergent wind in the upper troposphere indicates the ascending motion, while the positive velocity potential combined with the convergent wind indicates the descending
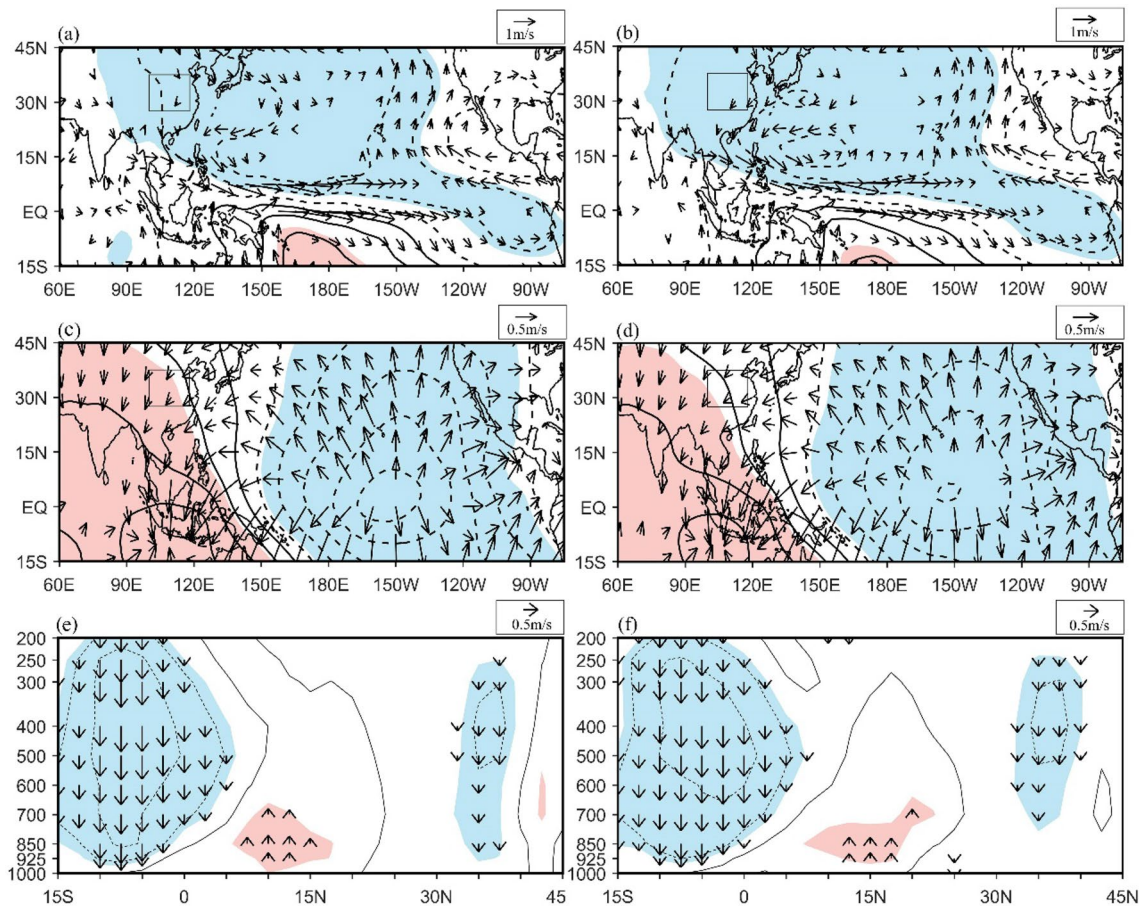

Fig. 2 Regressions of the anomalous JJA 850-hPa streamfunction (contours; 10^6 s^{-1}) and rotational winds (arrows; m s^{-1}) onto **a** the simultaneous JJA Niño3.4 index and **b** the following DJF Niño3.4 index during 1960-2014. **c**, **d** Same as **a** and **b**, but for the anomalous JJA 200-hPa velocity potential (contours; 10^6 m^2 s^{-1}) and

divergent winds (arrows; m s^{-1}). **e**, **f** Same as **a** and **b**, but for the anomalous JJA vertical winds averaged over 100° E–118° E (contours and arrows; 10^{-2} Pa s^{-1}). The shaded areas and arrows are at a significance level of $p < 0.1$. Wind speeds less than 0.15 m s^{-1} are not shown

motion. The results exhibit prominent ascending motions over the central and eastern Pacific and descending motions over the Maritime continent, indicating a weakened Walker circulation under the El Niño condition. The suppressed convection over the Maritime continent associated with the weakened Walker circulation would induce a weakened regional Hadley circulation (Wang 2002a, b, 2019; Yuan and Yang 2012). The JJA vertical wind anomalies regressed onto the simultaneous JJA and the following DJF Niño3.4 indices can further demonstrate this. Indeed, the suppressed convection over the Maritime continent is accompanied with an anomalous ascending motion north of the equator (Fig. 2e, f), which could induce an anomalous cyclone over South China and thus weaken the EASM (Fig. 2a, b). As a result, the developing El Niño significantly decreases the CCSP.

Given that the El Niño-related SST anomaly pattern experiences an obvious interdecadal change with a shift of the maximum warm SST anomalies from the eastern Pacific to the central Pacific in recent three decades, the relationships between the developing El Niño and the CCSP anomalies might also undergo an interdecadal change. To explore this issue, we calculate both the correlations for the whole period and the 21-year moving correlations between the normalized time series of the CCSP index and the simultaneous JJA/following DJF Niño3.4 index (Fig. 3). During 1960–2014, the correlation coefficients of the CCSP index with the simultaneous JJA and the following DJF Niño3.4 indices are -0.23 ($p < 0.1$) and -0.36 ($p < 0.01$), respectively. The significant

correlation coefficients suggest that the relationship between the developing El Niño and the CCSP anomalies is evident for the whole period. However, the 21-year moving correlation coefficients of the CCSP anomalies with the simultaneous JJA and the following DJF Niño3.4 indices show that such a negative correlation is unstable, with an interdecadal change since the late 1980s. Specifically, both the 21-year moving correlations are insignificant during 1960–1988 (the previous epoch) but dramatically strengthened during 1989–2014 (the post epoch). This suggests that the significant correlation for the whole period is a result of the strengthened relationship between the developing El Niño and the CCSP anomalies since the late 1980s.

Such an interdecadal change is also clearly presented by the spatial distributions of the correlation coefficients between the JJA precipitation anomalies and the simultaneous JJA/following DJF Niño3.4 index during 1960–1988 and 1989–2014 (Fig. 4). In the previous epoch, the correlation coefficients are weak, with insignificant positive correlations in the southeast of the central China and weak negative correlations in the rest part of the central China (Fig. 4a, c). In contrast, in the post epoch, strong negative correlations dominate the central China with the maximum value of about -0.8 (Fig. 4b, d). It directly demonstrates that the central China is prone to suffer drought during the summer when an El Niño event is in its developing stage since the late 1980s.

Figure 5 presents the scatter plots between the JJA central China precipitation anomalies and the simultaneous

Fig. 3 a Interannual time series of the JJA central China summer precipitation (CCSP) index (dashed black line) and the simultaneous JJA Niño3.4 index (solid black line) during 1960–2014. The solid blue line denotes the 21-year moving correlation coefficients between the two. b Same as a, but for the JJA CCSP index (dashed black line) and the following DJF Niño3.4 index (solid black line). The dashed blue lines in each panel denote the significance levels of $p < 0.05$ and $p < 0.01$, respectively. All data are linearly detrended and standardized
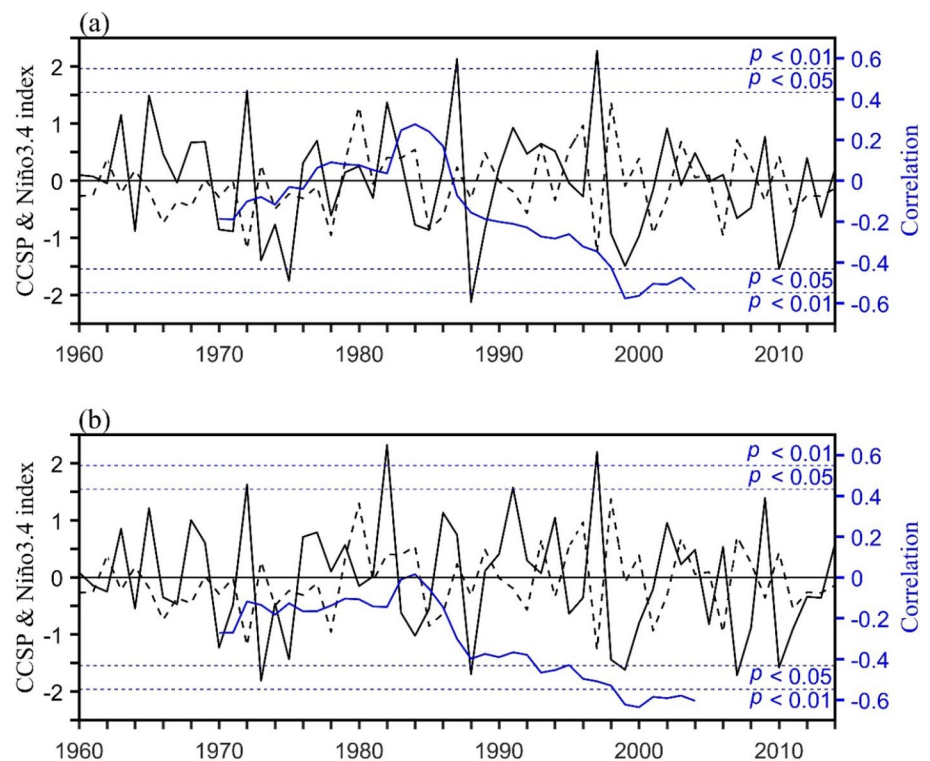
Fig. 4 Correlation coefficients of the JJA precipitation anomalies with the simultaneous JJA Niño3.4 index during the periods **a** 1960–1988 and **b** 1989–2014. **c** and **d** Same as **a** and **b**, but with the following DJF Niño3.4 index, respectively. The dots indicate that the correlations are at a significance level of $p < 0.05$. The box area in each panel denotes the region of the central China. All data are linearly detrended
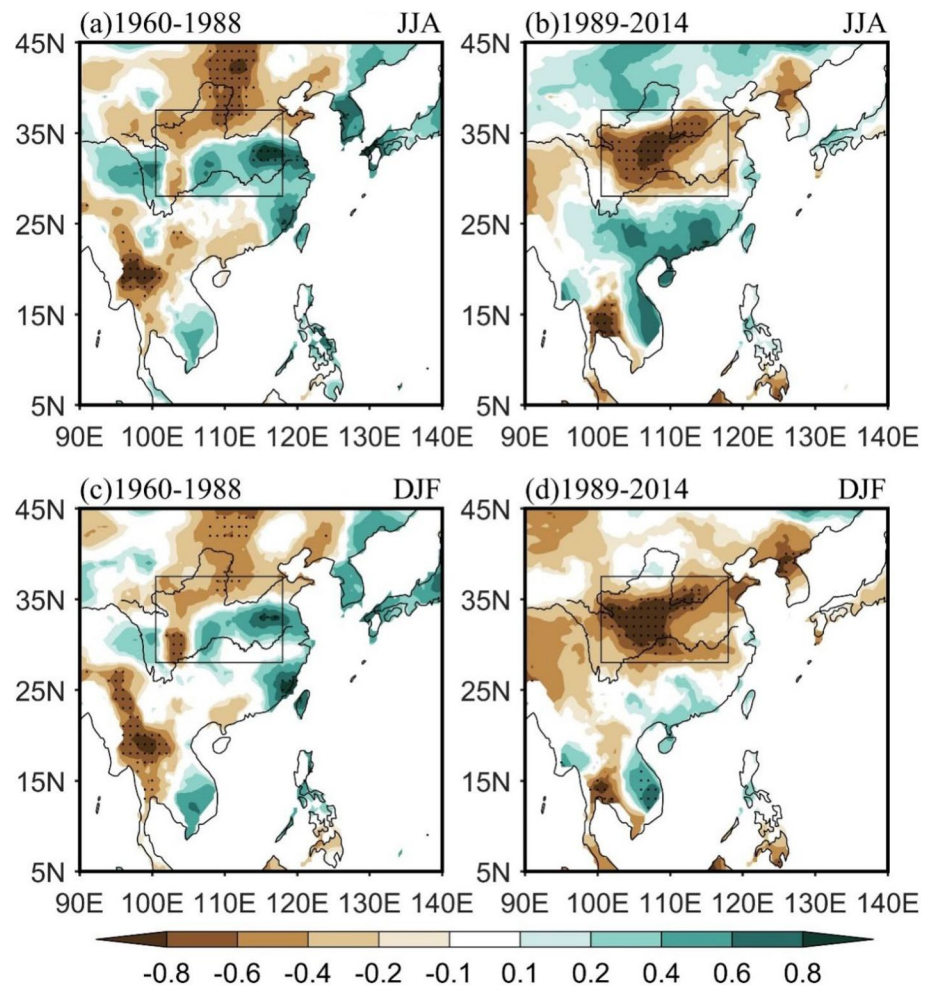
JJA/following DJF Niño3.4 index during 1960–1988 and 1989–2014. In the previous epoch, the correlation coefficient between the CCSP index and the simultaneous JJA/following DJF Niño3.4 index is low and not statistically significant (Fig. 5a, c), while this correlation in the post epoch is dramatically strengthened with a correlation coefficient of $-0.51/-0.56$ at a significance level of $p < 0.01$ (Fig. 5b, d). This further demonstrates that the El Niño's impact on the CCSP in the developing summer has strengthened since the late 1980s.

Figure 6 compares the correlation coefficients of the CCSP index with the SST anomalies from the simultaneous JJA to the following DJF between the previous and the post epochs. In the previous epoch, the CCSP exhibits insignificant correlations with the tropical Pacific SST anomalies from JJA to DJF (Fig. 6a–c). By contrast, the correlations of the CCSP with the tropical Pacific SST anomalies are much stronger in the post epoch, with statistically significant negative correlations dominating the region of the equatorial central Pacific during the simultaneous JJA and spreading into the equatorial eastern Pacific in the following SON and DJF (Fig. 6d–f). This suggests that the CCSP anomalies

are closely associated with the development of the El Niño events in the post epoch. The distinct correlation patterns in the Indian Ocean between the previous and post epochs also witness this changed relationship. According to the previous studies (Chowdary and Gnanaseelan 2007; Du et al. 2009; Xie et al. 2010, 2016; Wu et al. 2021), the variabilities of the Indian Ocean SST are closely associated with the El Niño events. With the development of El Niño, there are easterly wind anomalies over the equatorial Indian Ocean through Walker circulation adjustment, which maintain a negative wind curl over the southeast Indian Ocean and force downwelling Rossby waves propagating to the west (Xie et al. 2002; Du et al. 2009). As El Niño matures in winter, the enhanced solar radiation would cause the cool southeast Indian Ocean (a result of the seasonally upwelling off Java and Sumatra) to warm (Chowdary and Gnanaseelan 2007; Du et al. 2009), while the westward propagated Rossby waves would contribute to strengthened warming in the southwest Indian Ocean (Xie et al. 2002; Du et al. 2009). As a result, there is a charging process of the Indian Ocean SST with a dipole mode in autumn changing into a basin mode in the El Niño maturing winter. Such charging process

Fig. 5 Scatterplots of the CCSP index with the simultaneous JJA Niño3.4 index during the periods **a** 1960–1988 and **b** 1989–2014, respectively. **c** and **d** Same as **a** and **b**, but with the following DJF Niño3.4 index. Black lines and *r* in each panel denote linear fit and the correlation coefficient between the CCSP index and the Niño3.4 index, respectively. All data are linearly detrended and standardized
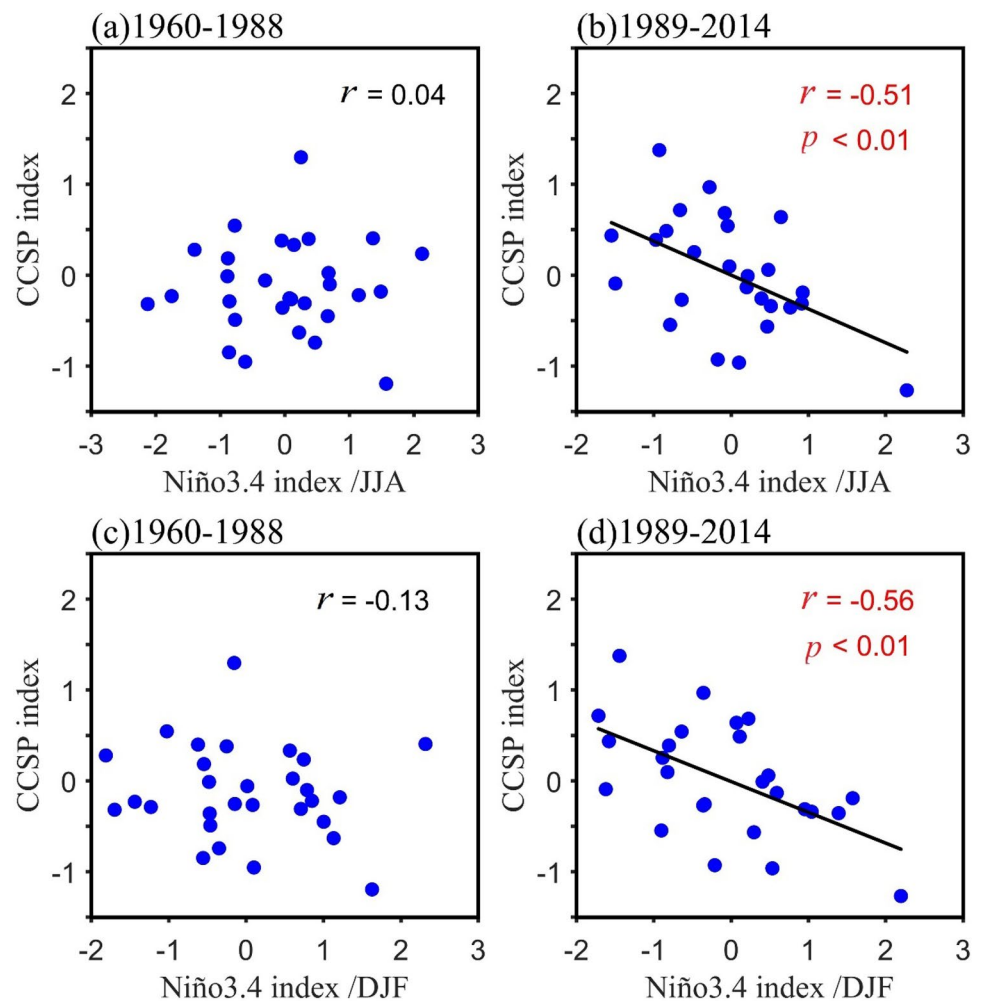
of the Indian Ocean is robust in the correlation pattern of the CCSP index with the SST anomalies from the simultaneous summer to the following winter during the post epoch (Fig. 6e, f). While that in the previous epoch is not shown (Fig. 6b, c). All of these confirm that there is a strengthened relationship between the developing El Niño and the CCSP anomalies since the late 1980s.

4 Possible mechanisms for the strengthening influence of El Niño

4.1 Interdecadal change in the El Niño intensities

The El Niño intensity can be expected to exert a great impact on the regional climate. A stronger El Niño event tends to have a larger effect on the East Asian summer climate (Wang et al. 2017). For example, the supper strong 1997/1998 El Niño event induces a devastating flood during the summer of 1998 over the Yangtze River basin, causing huge casualties and economic losses in the region (Huang et al. 1998; Zhou

et al. 2005; Xue and Liu 2008; Jiang et al. 2010). Therefore, we first examine the interdecadal variation of the El Niño intensities. Figure 7 displays the 21-year moving standard deviations of the JJA Niño3.4, Niño3 and Niño4 indices, together with that of the 21-year moving correlation coefficients of the CCSP anomalies with the simultaneous JJA and the following DJF Niño3.4 indices. The standard deviation of the Niño3.4 index as well as that of the Niño3 and Niño4 indices denotes the intensity of the ENSO events, which are largely consistent in the variations. However, they all exhibit weak correlations with the developing El Niño-CCSP relationship. Specifically, the correlation coefficients between the moving standard deviation of the JJA Niño3.4 index and the two moving correlations are -0.25 and -0.22 ($p > 0.1$), respectively. For the correlations of the moving standard deviation of the JJA Niño3/ Niño4 index with the two moving correlations, they are $-0.28/-0.27$ and $-0.24/-0.17$ ($p > 0.1$), respectively. This illustrates that the dramatical interdecadal change of the El Niño-CCSP relationships since the late 1980s cannot be explained by that of the El Niño intensities.
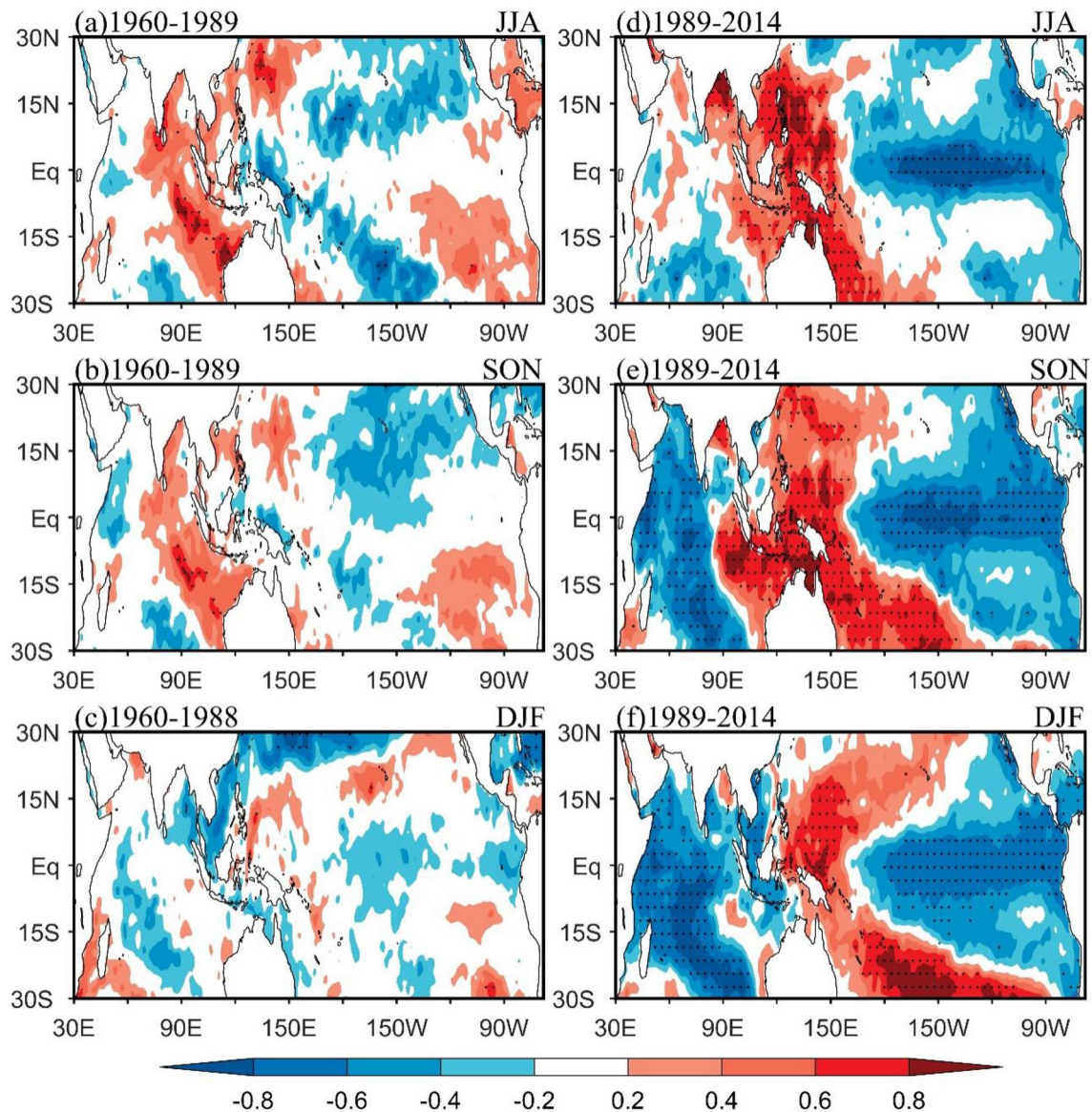
Fig. 6 Correlation coefficients of the CCSP index with **a** the simultaneous JJA, **b** the following autumn [September–October–November (SON)] and **c** the following DJF SST anomalies during the period 1960–1988. **d–f** Same as **a–c**, but for the period 1989–2014. The dots indicate that the correlations are at a significance level of $p < 0.05$. All data are linearly detrended

4.2 Interdecadal change in the El Niño-related SST anomaly patterns

The relationship between the developing El Niño and the CCSP anomalies strengthens since the late 1980s. Notably, the frequency of the CP El Niño also increases since the late 1980s (Ashok et al. 2007; Yeh et al. 2009; Lee and McPhaden 2010). According to the statistics, there are two CP El Niño events and six EP El Niño events in the previous epoch. In contrast, there are five CP El Niño events and two EP El Niño events in the post epoch (Table 1). Obviously, the CP El Niño events appear more frequently than the EP El Niño events in the post epoch. Previous studies

reported that the CP El Niño could exert more significant effect on the East Asian climate than the EP El Niño in the developing summer (Weng et al. 2007; Yuan and Yang 2012; Yuan et al. 2012; Chen et al. 2019). Therefore, the changed El Niño-related SST anomaly pattern might be the reason for the interdecadal change in the relationship between the developing El Niño and the CCSP since the late 1980s.

To demonstrate this, here we conduct composite analyses based on the El Niño developing years of the two epochs. Note that there is one super strong El Niño event (1982/1983 and 1997/1998) in the previous and post epochs, respectively. To remove the influence of the super strong El Niño events, we exclude the years of 1982 and 1997 in the
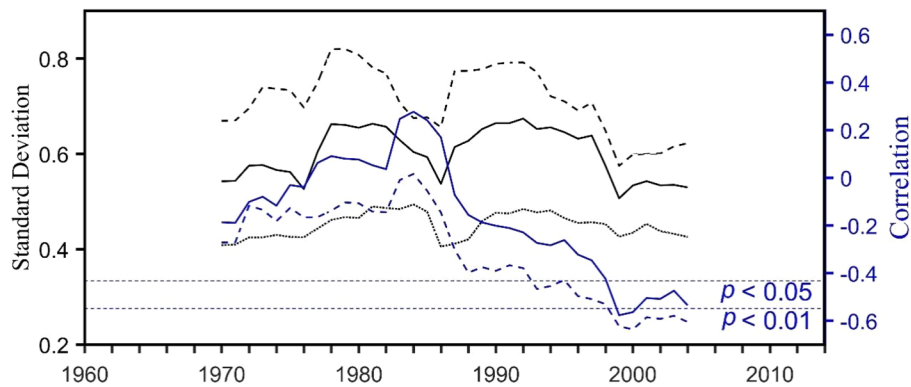
Fig. 7 The 21-year moving standard deviations (SDs) of the JJA Niño3.4 index (solid black line), Niño3 index (dashed black line) and Niño4 index (dotted black line) during 1960–2014. The solid (dashed) blue line is the 21-year moving correlations between the CCSP index and the simultaneous JJA (following DJF) Niño3.4 index during 1960–2014. The straight dashed blue lines denote the significance levels of $p < 0.05$ and $p < 0.01$, respectively. All data are linearly detrended and standardized

composite analyses. Figure 8 displays the evolutions of the composite SST anomalies from MAM to SON for the El Niño developing years during 1960–1988 and 1989–2014. In both epochs, the SST anomalies in the tropical Pacific feature a developing process of the El Niño event from MAM to SON. But the SST anomaly patterns in the tropical Pacific are quite different between the previous and post epochs. Specifically, in the previous epoch, SST anomalies in the tropical Pacific feature a dipole mode with cooling in the west and warming in the east. With the development of the El Niño events, the NWP SST anomalies get cooler. And the warm SST anomalies of the developing El Niño gradually grow from MAM to SON with the maximum warm SST anomalies located in the tropical eastern Pacific. (Fig. 8a–c). In contrast, in the post epoch, such dipole SST anomaly pattern only appears in SON. And the warm SST anomalies in the tropical Pacific mainly develop in JJA and strengthen in SON, with stronger warming in the central Pacific region than the eastern Pacific region (Fig. 8d–f). Obviously, in the developing summer of El Niño, there are remarkable discrepancies in the SST anomaly pattern between the previous and the post epochs with an evident interdecadal shift of the maximum warm SST anomalies from the eastern Pacific to the central Pacific.

In Fig. 9, we further display the monthly evolutions of the Niño3 and Niño4 indices for the El Niño developing years between the previous and the post epochs. In the Niño3 region, the SST anomalies in the previous epoch are stronger than that in the post epoch. In particular, in the middle and late JJA, the Niño3 SST anomalies in the previous epoch are more than twice of that in the post epoch (Fig. 9a). By contrast, in the Niño4 region, the situation is opposite. During JJA, significant warming only occurs in the post epoch (Fig. 9b). All these indicate that the anomalous warming centers of the developing El Niño events are quite different

between the previous and the post epochs, which mainly locate in the eastern Pacific during the previous epoch but in the central Pacific during the post epoch. Furthermore, the changed El Niño-related SST anomaly pattern since the late 1980s also implies that the regional atmospheric circulation responses to El Niño would also undergo an interdecadal shift between these two epochs.

4.3 Interdecadal change in the El Niño-induced atmospheric circulation anomalies

Figure 10 shows the composite SST as well as the 850-hPa wind and streamfunction anomalies for the El Niño developing summer during 1960–1988 and 1989–2014. In both epochs, anomalous cyclonic circulations, along with the negative streamfunction contours, appear over the NWP, as a Gill-type Rossby wave response to the equatorial Pacific SST warming. However, corresponding to the distinct SST anomaly pattern between the previous and post epochs, the locations of the two cyclones also show large discrepancies for the two subperiods (Fig. 10). During 1960-1988, the anomalous cyclone locates between 120° E and 170° E, with its west rim east of South China (Fig. 10a). In contrast, during 1989–2014, such an anomalous cyclone locates between 100° E and 160° E, with its north part located over South China (Fig. 10b). Clearly, the low-level atmospheric circulation anomalies extend westward from the previous epoch to the post epoch (Fig. 10), physically consistent with the westward shift of the maximum warm SST anomalies from the eastern Pacific to the central Pacific (Figs. 8, 9). Such a westward extension of the atmospheric circulation anomalies, with an anomalous cyclone reaching South China in the post epoch, would weaken the southwest monsoon and affect the water vapor budget of the central China, and thus
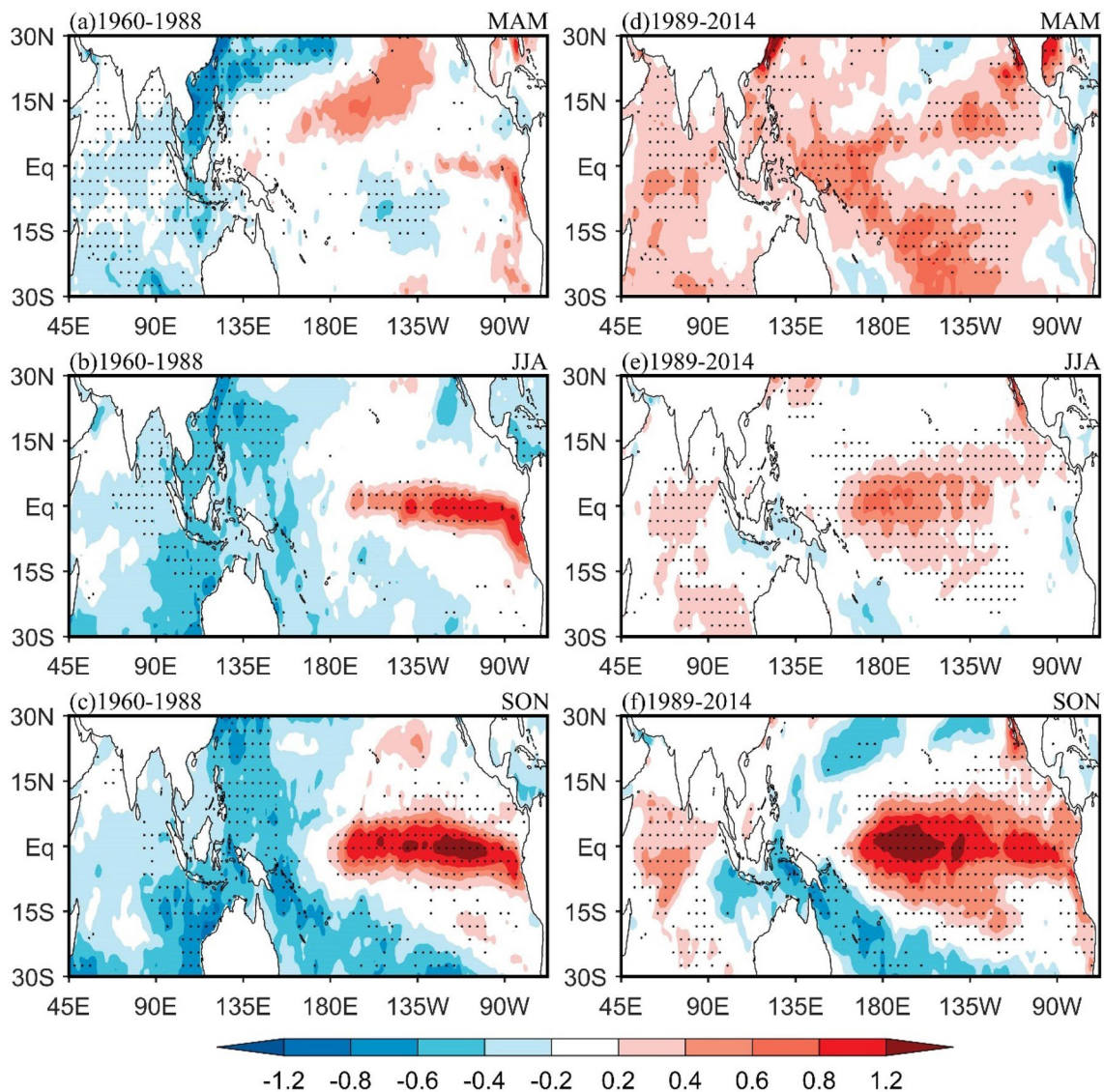
Fig. 8 Composite SST anomalies (°C) of the developing **a** spring [March–April–May (MAM)], **b** JJA and **c** SON for the El Niño events during 1960-1988. **d–f**, Same as **a–c**, but for the period 1989-2014. The dots in each panel indicate that the correlations are at a significance of $p < 0.05$

explain why there are prominent CCSP anomalies during the El Niño developing stage since the late 1980s.

How do the different SST anomaly patterns in the tropical Pacific during the previous and the post epochs result in distinct low-level atmospheric circulation responses over South China? According to the previous studies, SST warming in the tropical Pacific can directly exert an anomalous cyclone propagating to the west as a Gill-type Rossby wave response (Wang et al. 2013, 2017; Chen et al. 2014; Li et al. 2017b). Corresponding to the westward shift of the warm SST anomalies in the tropical Pacific, the Gill-type atmospheric circulation responses also extend westward. As a result, the anomalous cyclone in the post epoch reaches South China while that in the previous epoch is far away from South China (Fig. 10).

Meanwhile, the adjustment of the Walker circulation also plays an important role. Figure 11 shows the composite JJA 200-hPa velocity potential and divergent wind anomalies for the El Niño developing years during the previous and post epochs. In both epochs, the anomalous warm SST in the tropical Pacific anchors large-scale divergent motions over the central and eastern Pacific and convergent motions over the Indo-western Pacific, indicating a weakened Walker circulation (Fig. 11). However, as there are discrepancies in the El Niño SST anomaly patterns between the previous and post epochs, the upper-level divergent and convergent area also exhibits substantial differences. In response to the westward shift of the anomalous warming center in the tropical Pacific from the previous epoch to the post epoch, the anomalous Walker

Fig. 9 Composite evolutions of SST anomalies averaged in the **a** Niño3 region (5° S–5° N, 150° W–90° W) and **b** Niño4 region (5° S–5° N, 160° E–150° W) from the El Niño developing March to the decaying February during 1960–1988 and 1989–2014. The solid bars are at a significance level of $p < 0.05$. The months of June, July and August in each panel are boxed
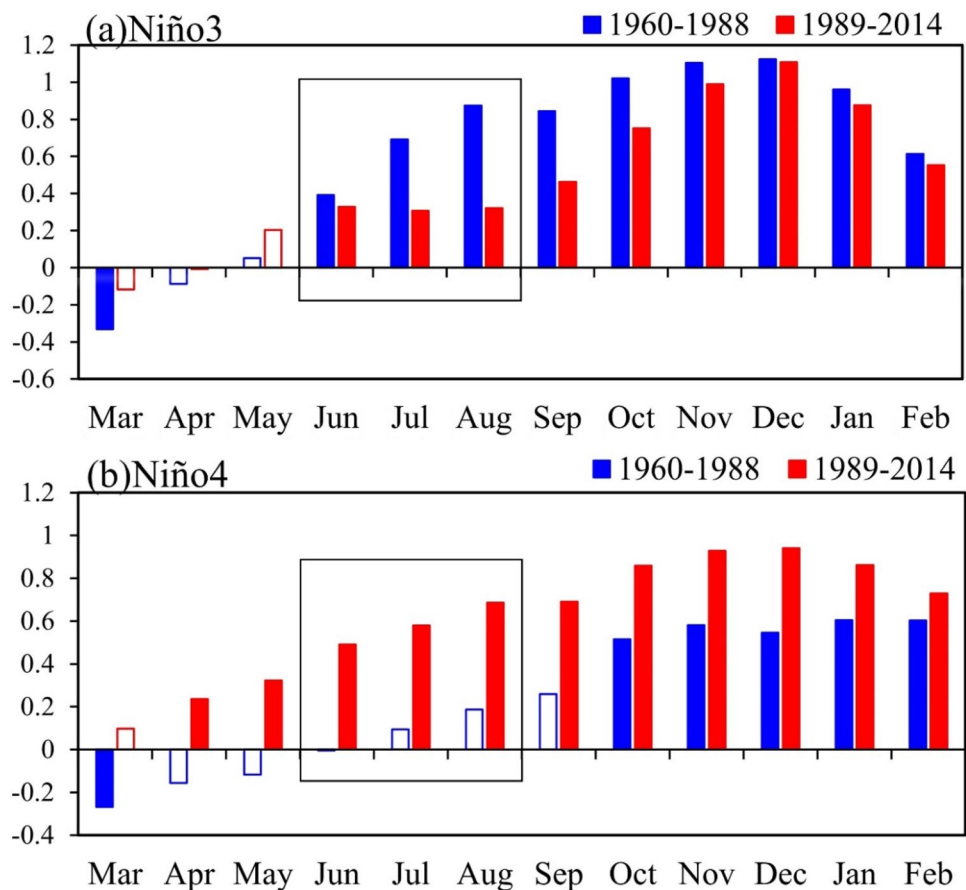

cell also shifts westward (Fig. 11). The sinking branch of the Walker circulation reaches to the Maritime Continent in the post epoch (Fig. 11b), while that in the previous epoch is weak and relatively shifts eastward (Fig. 11a). The suppressed convections with decreased precipitation (calculated by the precipitation rate) over the Indo-western Pacific in these two epochs also support this (Fig. 11).

Different locations of the suppressed convection over the Indo-western Pacific would further cause different Hadley circulation responses (Yuan and Yang 2012; Wang 2019). In Fig. 12, we display the composite JJA vertical wind anomalies averaged over 100° E–118° E for the El Niño developing years during the previous and post epochs. Obviously, corresponding to the more significant anomalous descending motion over the Maritime continent in the post epoch, prominent anomalous ascending motion appears over South China (Fig. 12b). But in the previous epoch, such vertical motion over South China is weak and insignificant (Fig. 12a). The ascending motion is combined with the airflow convergence in the low-level. As a result, there are prominent cyclonic circulation anomalies over South China in the post epoch (Fig. 10b), while that in the previous epoch are not evident (Fig. 10a).

The different atmospheric circulation responses between the previous and post epochs would certainly cause different water vapor budget over the central China. Figure 13 shows the composite JJA vertically integrated (1000–300-hPa) water vapor flux and its divergence for the El Niño developing years during the two epochs. The vertically integrated water vapor flux resembles the low-level circulation pattern to a large extent, indicating that the low-level wind plays an important role in transporting the moisture. In the post epoch, the significant cyclonic circulation anomalies over South China, with anomalous northeasterly winds in the west, weaken the prevailing southwest monsoon and result in divergence over the central China. As a result, there is a deficit in the CCSP during the El Niño developing stage (Fig. 13b). While in the previous epoch, there are insignificant circulation anomalies over China, and thus inapparent water vaper transport from the ocean to the central China (Fig. 13a). This explains why the relationship in the El Niño-CCSP is weak during this period.

Finally, we present the relationships among the tropical Pacific SST anomalies, the South China cyclonic circulation anomalies and the CCSP anomalies for the previous and post epochs, respectively (Fig. 14), which can help us better

Fig. 10 Composite anomalies of the JJA SST (shaded; °C), 850-hPa winds (arrows; m s^{-1}) and 850-hPa streamfunction (contours; 10^7 s^{-1}; purple line denotes the zero contour) for the El Niño developing years during **a** 1960–1988 and **b** 1989–2014. The dots indicate that the composited SST anomalies are at a significance level of $p < 0.05$. The shown arrows are presented with the zonal or meridional component of the wind anomalies exceeding the significance level of $p < 0.1$. Wind speeds less than 0.5 m s^{-1} are not shown
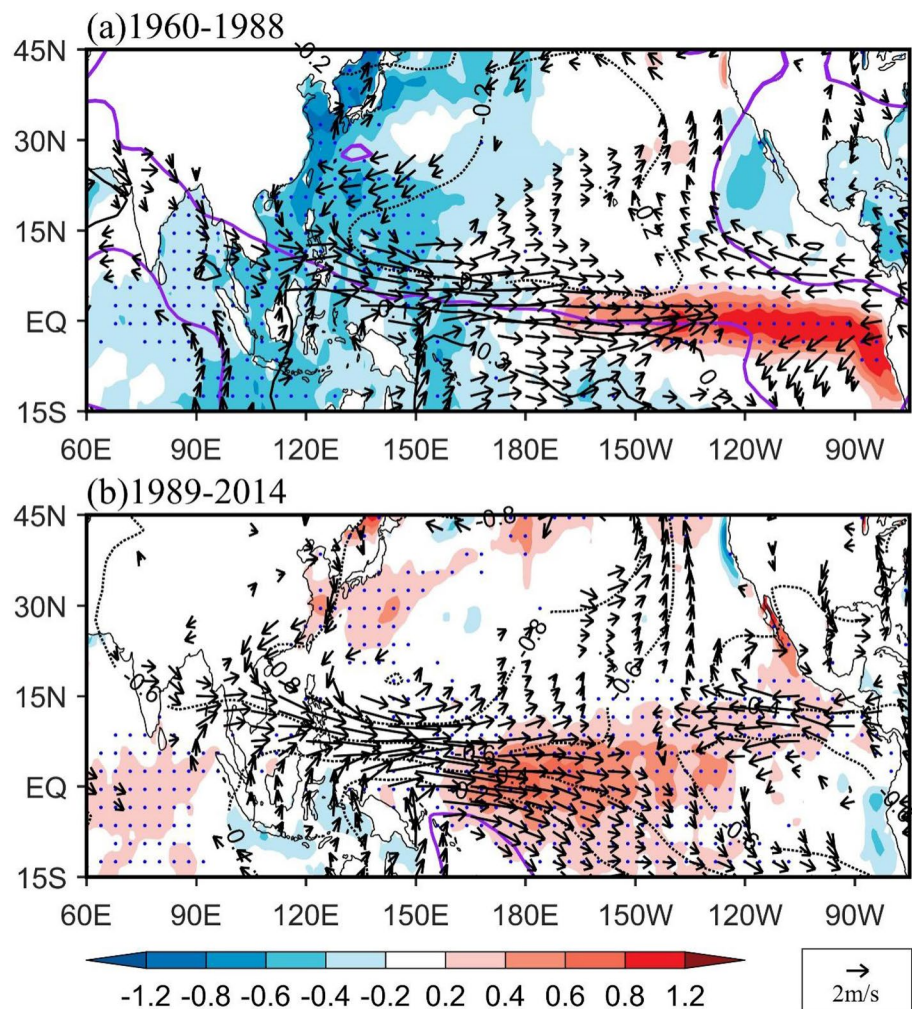
understand the strengthened influences of the developing El Niño on the CCSP since the late 1980s. The CP El Niño events occur more frequently since the late 1980s, leading to an interdecadal shift of the El Niño-related SST anomaly pattern from the eastern Pacific to the central Pacific (Figs. 9, 10). The changed SST anomaly pattern further results in a different location of low-level cyclonic circulations over the NWP, with an anomalous cyclone reaching to South China in the post epoch, while that in the previous epoch locates in the east of South China (Fig. 10). When denoting the South China cyclone index as the difference of the 850-hPa zonal wind anomalies averaged between the regions of 20° N–30° N, 100° E–120° E and 5° N–15° N, 100° E–130° E, the correlation coefficient between the JJA Niño3.4 index and the simultaneous South China cyclone index is statistically insignificant in the previous epoch (Fig. 14a), while that in the post epoch is greatly strengthened, with a correlation coefficient of 0.52 at a significance level of $p < 0.01$ (Fig. 14c). Such an anomalous cyclone over South China greatly prevents the southwest monsoon from transporting water vapor to the north (Fig. 13b). As a result, decreased

precipitation occurs over the central China in the post epoch (Figs. 11b, 13b). The correlation between the South China cyclone index and CCSP index in the post epoch further supports this, with a correlation coefficient of − 0.75 at a significance level of $p < 0.001$ (Fig. 14d). However, this correlation is not statistically significant in the previous epoch (Fig. 14c).

5 Summary and discussion

The variation of the CCSP is of great social and economic significance for this densely populated region. The present study identifies that the El Niño events strongly modulate the CCSP, with negative precipitation anomalies locate in the region of the central China during the summertime when an El Niño event is in its developing phase. However, such a negative correlation between the developing El Niño and the CCSP anomalies is unstable, exhibiting an interdecadal change around 1989, with

Fig. 11 Composite anomalies of the JJA 200-hPa velocity potential (contours; 10^6 m^2 s^{-1}; purple line denotes the zero contour), divergent wind (arrows; m s^{-1}) and simultaneous JJA precipitation (calculated by precipitation rate; shaded; mm month^{-1}) for the El Niño developing years during **a** 1960–1988 and **b** 1989–2014. The shaded areas are at a significance level of $p < 0.2$. Wind speeds less than 0.5 m s^{-1} are not shown. The box area in each panel denotes the region of the central China
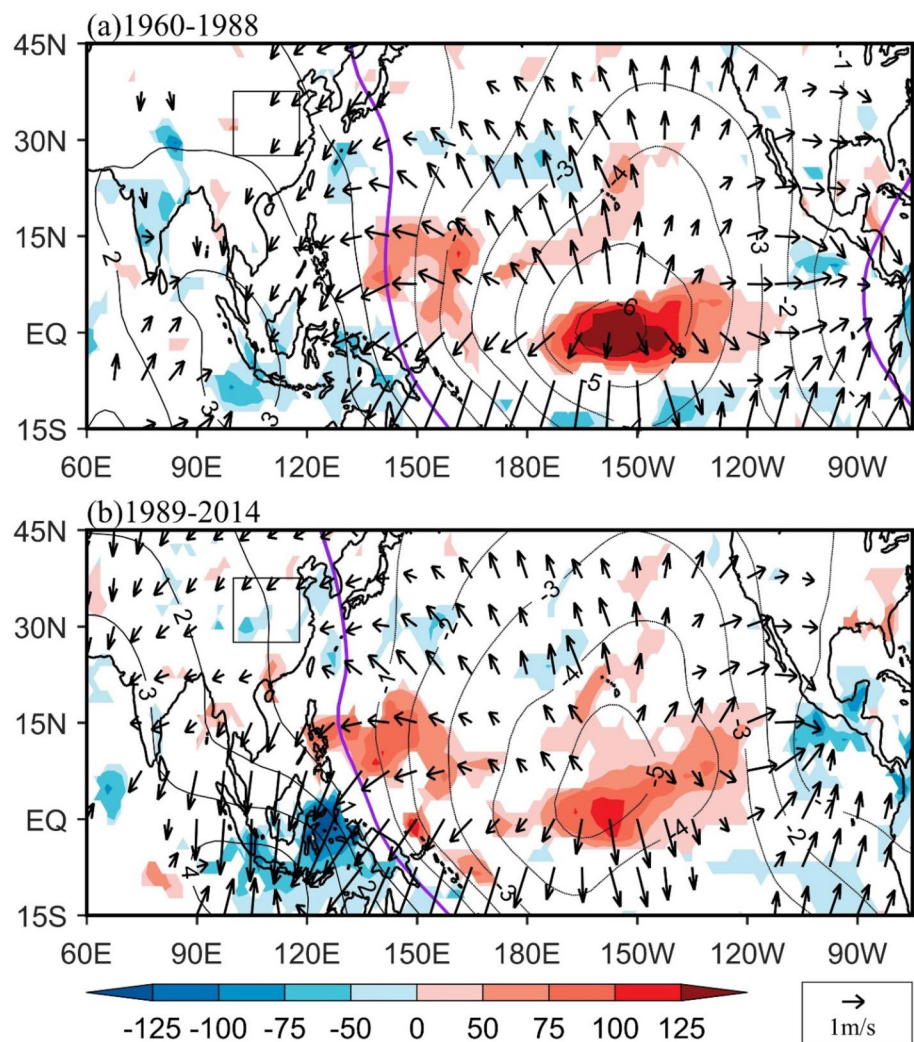
weak correlation during the previous epoch (1960–1988) but dramatically strengthened correlation during the post epoch (1989–2014).

Further analyses suggest that the interdecadal change in the El Niño–CCSP relationships is mainly attributed to that of the El Niño SST anomaly patterns. In the previous epoch, the anomalous warm SST center in the El Niño developing summer locates in the equatorial eastern Pacific, while it shifts to the central Pacific in the post epoch. The changed El Niño SST anomaly pattern in the tropical Pacific results in different atmospheric circulation responses. Corresponding to the westward shift of the SST anomaly patterns from the previous epoch to the post epoch, the El Niño-related Walker circulations also extend westward. This leads to anomalous descending motions over the Maritime Continent and further emanates an off-equatorial anomalous low-level cyclone covering South China. The anomalous cyclone prevents the southwest monsoon from delivering the moisture to the north, reducing precipitation in the central China. However, such an anomalous cyclone only appears over the

east of South China during the previous epoch, thus having no significant effect on the CCSP.

The present study highlights that the increased occurrences of the CP El Niño events could lead to a strengthened impact of El Niño on the CCSP in the developing stage. It is reported that such increased occurrences of the CP El Niño originate from a warmer Atlantic due to the positive phase of Atlantic multidecadal oscillation and the global warming trends (McGregor et al. 2014; Li et al. 2016b; Cai et al. 2019). However, even there is a better understanding of the physical mechanisms of the El Niño events, accurate prediction of the El Niño events in the coupled general circulation models still suffers great challenges (Barnston et al. 2012; Li and Xie 2014; Li et al. 2016a, 2017a; Newman and Sardeshmukh 2017; Petrova et al. 2017), particularly for CP El Niño events, as their evolution and climate feedbacks tend to be more difficult to forecast than those of EP El Niño events (Jeong et al. 2012; Wang et al. 2019). This potentially limits the prediction skill in the El Niño-related atmospheric teleconnections in

Fig. 12 Composite JJA vertical wind anomalies (contours and arrows; 10^{-2} Pa s^{-1}; the shaded areas are at a significance level of $p < 0.1$) averaged over 100° E–118° E for the El Niño developing years during **a** 1960–1988 and **b** 1989–2014. The shown arrows are presented with the vertical wind anomalies exceeding the significance level of $p < 0.1$. The arrows with wind speed less than 0.2 m s^{-1} are removed
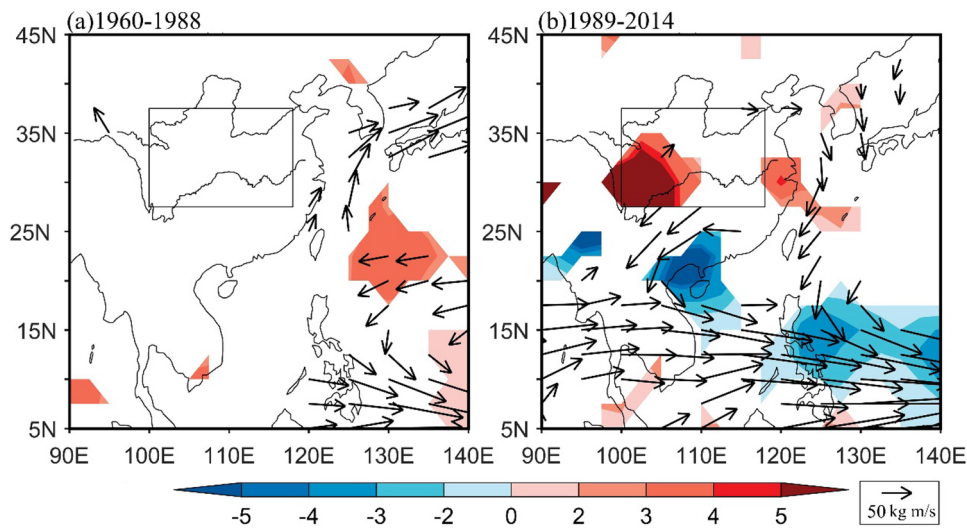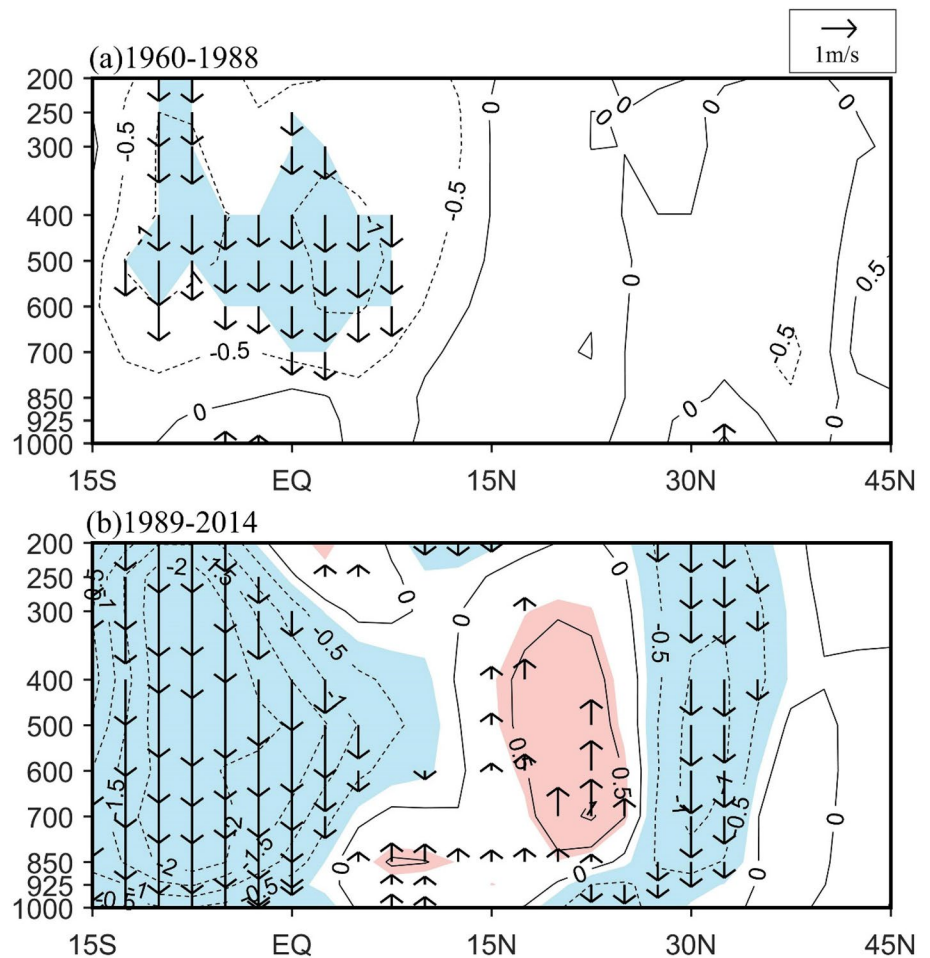

Fig. 13 Composite anomalies of the JJA water vapor flux integrated from 1000 to 300-hPa (arrows; kg m^{-1} s^{-1}) and its divergence (shaded; 10^{-5} kg m^{-2} s^{-1}) for the El Niño developing years during **a** 1960–1988 and **b** 1989–2014. The shaded areas are at a significant level of $p < 0.2$. The shown arrows are presented with the zonal or meridional component of the water vapor flux anomalies exceeding the significance level of $p < 0.1$. The arrows with water vapor flux anomalies less than 5 kg m^{-1} s^{-1} are not shown. The box area in each panel denotes the region of the central China

Fig. 14 Scatterplots of **a** the JJA Niño3.4 index with the simultaneous JJA cyclone index (defined as the difference of the 850-hPa zonal wind anomalies between 20° N–30° N, 100° E–120° E and 5° N–15° N, 100° E–130° E) and **b** the JJA cyclone index with the simultaneous CCSP index for the period 1960–1988. **c** and **d** Same as **a** and **b**, but for the period 1989–2014. All data are linearly detrended and standardized
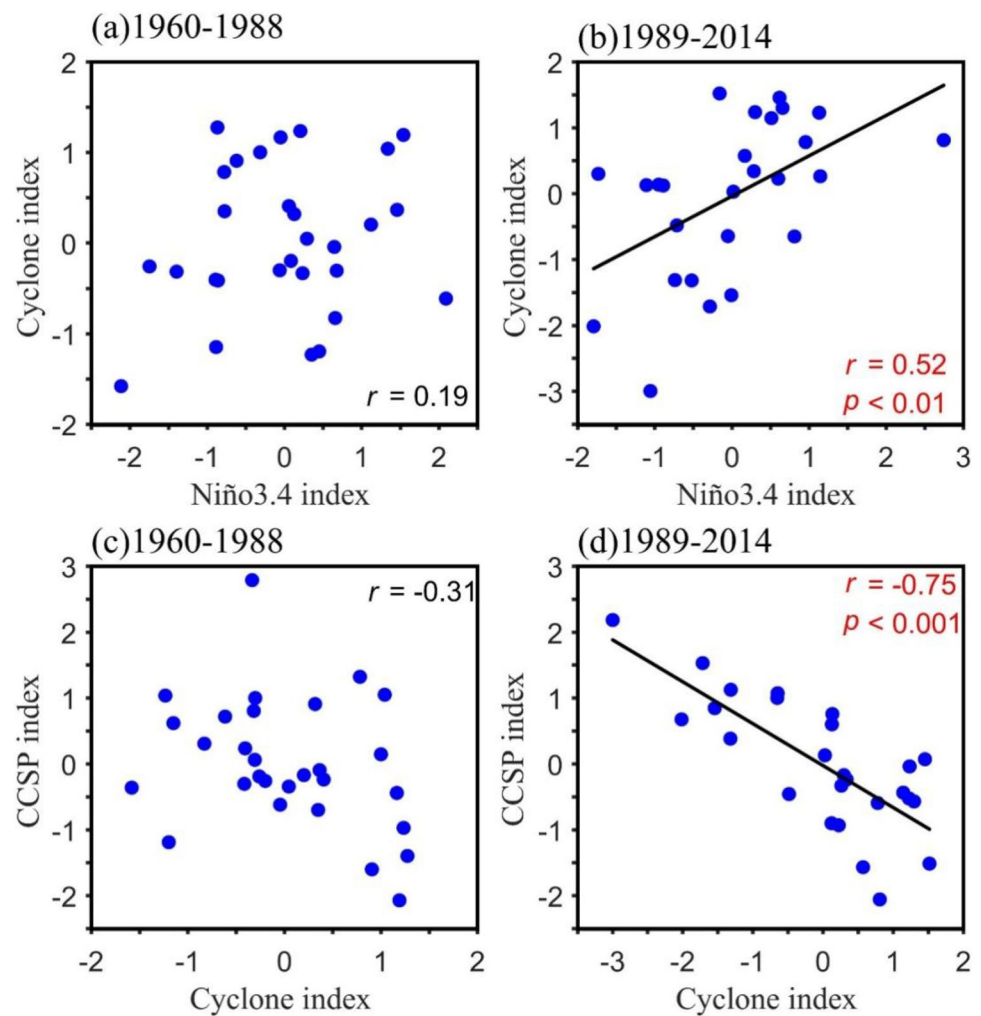
the recent epoch (Zou et al. 2014; Feng et al. 2019; Wang et al. 2019; Yu et al. 2020; Wu et al. 2020; Chen et al. 2021), such as the CCSP. This means that an improved El Niño prediction is a priority for the reliable prediction of the CCSP. Owing to the high dependence of the central China on summer precipitation, the potential benefits of an improved seasonal prediction of the CCSP are enormous for the local people's livelihood, including the agriculture, ecosystems, water resources, economies, and health.

With a more frequent occurrence of the CP El Niño events, is the relationship between the decaying El Niño and the CCSP anomalies also changed since the late 1980s? The mechanisms of El Niño influencing the East Asian summer climate in the decaying stage are rather complex. It is mediated not only by the intensity and location of the El Niño events, but also the decaying pace of the El Niño events (Feng et al. 2010; Xie et al. 2010; Chen et al. 2016; Wang et al. 2017; Zhou et al. 2019; Wu et al. 2020). Whether/how the changing El Niño activity also modulates the relationship between the decaying El Niño and the CCSP anomalies needs further exploration in the future work.

References

An SI, Wang B (2001) Mechanisms of locking of the El Niño and La Niña nature phases to boreal winter. J Clim 14:2164–2176

Ashok K, Behera KS, Rao SA et al (2007) El Niño Modoki and its possible teleconnection. J Geophys Res 112:C11007. https://doi.org/10.1029/2006JC003798

Barnston AG, Tippett MK, L'Heureux ML et al (2012) Skill of real-time seasonal ENSO model predictions during 2002–11: is our capability increasing? Bull Am Meteorol Soc 93:631–651

Cai W, Wu L, Lengaigne M et al (2019) Pantropical climate interactions. Science 363:1–11

Cao Q, Hao ZC, Zhou JW et al (2019) Impacts of various types of El Niño–Southern Oscillation (ENSO) and ENSO Modoki on the rainy season over the Huaihe river basin. Int J Climatol 39:2811–2824

Chang CP, Zhang Y, Li T (2000) Interannual and interdecadal variations of the East Asian summer monsoon and tropical Pacific SSTs. Part I: role of the subtropical ridge. J Clim 13:4310–4325

Chang CP, Zhang Y, Li T (2000) Interannual and interdecadal variations of the East Asian summer monsoon and tropical Pacific SSTs. Part II: meridional structure of the monsoon. J Clim 13:4326–4340

Chen W (2002) Impacts of El Niño and La Niña on the cycle of the East Asian winter and summer monsoon (in Chinese). Chin J Atmos Sci 26:595–610

Chen TC, Wang SY, Huang WR, Yen MC (2004) Variation of the East Asian summer monsoon rainfall. J Clim 17:744–762

Chen ZS, Wen ZP, Wu RG et al (2014) Influence of two types of El Niño on the East Asian climate during boreal summer: a numerical study. Clim Dyn 43:469–481

Chen Z, Wen Z, Wu R et al (2016) Relative importance of tropical SST anomalies in maintaining the western North Pacific anomalous anticyclone during El Niño to La Niña transition years. Clim Dyn 46:1027–1041

Chen Z, Du Y, Wen Z et al (2018) Indo-Pacific climate during the decaying phase of the 2015/16 El Niño: role of southeast tropical Indian Ocean warming. Clim Dyn 50:4707–4719

Chen W, Wang L, Feng J et al (2019) Recent progress in studies of the variability and mechanisms of the East Asian monsoon in a changing climate. Adv Atmos Sci 36:887–901

Chen MY, Chang TH, Lee CT et al (2021) A study of climate model responses of the western Pacific subtropical high to El Niño diversity. Clim Dyn 56:581–595

Chiang JCH, Kong W, Wu CH, Battisti DS (2020) Origins of East Asian summer monsoon seasonality. J Clim 33:7945–7965

Chowdary JS, Gnanaseelan C (2007) Basin-wide warming of the Indian Ocean during El Niño and Indian Ocean dipole years. Int J Climatol 27:1421–1438

Deser C, Alexander MA, Xie SP, Phillips AS (2010) Sea surface temperature variability: patterns and mechanisms. Ann Rev Mar Sci 2:115–143

Ding Y (2007) The variability of the Asian summer monsoon. J Meteorol Soc Japan 85B:21–54

Ding Y, Chan JCL (2005) The East Asian summer monsoon: an overview. Meteorol Atmos Phys 89:117–142

Ding Y, Liu Y, Hu ZZ (2021) The record-breaking Meiyu in 2020 and associated atmospheric circulation and tropical SST anomalies. Adv Atmos Sci 6:1–14

Du Y, Xie SP, Huang G, Hu KM (2009) Role of air-sea interaction in the long persistence of El Niño-induced North Indian Ocean warming. J Clim 22:2023–2038

Feng J, Chen W, Tam CY, Zhou W (2010) Different impacts of El Niño and El Niño Modoki on China rainfall in the decaying phase. Int J Climatol 31:2091–2101

Feng J, Chen W, Gong HN et al (2019) An investigation of CMIP5 model biases in simulating the impacts of central Pacific El Niño on the East Asian summer monsoon. Clim Dyn 52:2631–2646

Feng Y, Chen XY, Tung KK (2020) ENSO diversity and the recent appearance of central Pacific ENSO. Clim Dyn 54:413–433

Gao CJ, Li G, Xu B, Li XY (2020a) Effect of spring soil moisture over the Indo-China Peninsula on the following summer extreme precipitation events over the Yangtze River basin. Clim Dyn 54:3845–3861

Gao CJ, Li G, Chen HS, Yan H (2020b) Interdecadal change in the effect of spring soil moisture over the Indo-China Peninsula on the following summer precipitation over the Yangtze river basin. J Clim 33:7063–7082

Gao CJ, Li G, Xu B (2020c) Weakening influence of spring soil moisture over the Indo-China Peninsula on the following summer Mei-yu front and precipitation extremes over the Yangtze river basin. J Clim 33:10055–10072

Harris I, Jones PD, Osborn TJ, Lister DH (2014) Updated high-resolution grids of monthly climatic observations-the CRU TS3.10 dataset. Int J Climatol 34:623–642

He C, Zhou T, Li T (2019) Weakened anomalous western North Pacific anticyclone during an El Niño-decaying summer under a warmer climate: dominant role of the weakened impact of the tropical Indian Ocean on the atmosphere. J Clim 32:213–230

He LQ, Hao X, Han TT (2021) The asymmetric impacts of ENSO Modoki on boreal winter climate over the Pacific and its rim. Clim Dyn 56:29–44

Hu K, Xie SP, Huang G (2017) Orographically anchored El Niño effect on summer rainfall in central China. J Clim 30:10037–10045

Hu K, Huang G, Xie SP, Long SM (2019) Effect of the mean flow on the anomalous anticyclone over the Indo-Northwest Pacific in post-El Niño summers. Clim Dyn 53:5725–5741

Hu K, Liu Y, Huang G et al (2020) Contributions to the interannual summer rainfall variability in the mountainous area of central China and their decadal changes. Adv Atmos Sci 37:259–268

Huang R, Wu Y (1989) The influence of ENSO on the summer climate change in China and its mechanisms. Adv Atmos Sci 6:21–32

Huang R, Xu Y, Wang P, Zhou L (1998) The features of the catastrophic flood over the Changjiang river basin during the summer of 1998 and cause exploration (in Chinese). Climatic Environ Res 3:300–313

Huang YY, Wang B, Li XF, Wang HJ (2018) Changes in the influence of the western Pacific subtropical high on Asian summer monsoon rainfall in the late 1990s. Clim Dyn 51:443–455

Jeong HI, Lee DY, Ashok K et al (2012) Assessment of the APCC coupled MME suite in predicting the distinctive climate impacts of two flavors of ENSO during boreal winter. Clim Dyn 39:475–493

Jiang T, Kundzewicz ZW, Su B (2010) Changes in monthly precipitation and flood hazard in the Yangtze river basin, China. Int J Climatol 28:1471–1481

Jiang WP, Li G, Wang GJ (2021) Effect of the El Niño decaying pace on the East Asian summer monsoon circulation pattern during post-El Niño summers. Atmosphere 12:1–13

Kalnay E et al (1996) The NCEP/NCAR 40-year reanalysis project. Bull Am Meteorol Soc 77:437–471

Karori MA, Li JP, Jin FF (2013) The asymmetric influence of the two types of El Niño and La Niña on summer rainfall over Southeast China. J Clim 26:4567–4582

Ke D, Guan ZY (2014) Regional mean daily precipitation extremes over central China during boreal summer and its relation with the anomalous circulation patterns (in Chinese). Acta Meteorol Sin 72(3):478–493

Kug JS, Jin FF, An SI (2009) Two types of El Niño events: cold tongue El Niño and warm pool El Niño. J Clim 22:1499–1515

Lau NC, Leetmaa A, Nath MJ, Wang HL (2005) Influences of ENSO-induced Indo-western Pacific SST anomalies on extratropical atmospheric variability during the boreal summer. J Clim 18:2922–2942

Lee T, McPhaden MJ (2010) Increasing intensity of El Niño in the central-equatorial Pacific. Geophys Res Lett 37:L14603. https://doi.org/10.1029/2010GL044007

Li XY, Lu RY (2020) Breakdown of the summertime meridional teleconnection pattern over the western North Pacific and East Asia since the early 2000s. J Clim 33:8487–8505

Li G, Xie SP (2014) Tropical biases in CMIP5 multimodel ensemble: the excessive equatorial Pacific cold tongue and double ITCZ problems. J Clim 27:1765–1980

Li XZ, Zhou W, Chen DL et al (2014) Water vapor transport and moisture budget over Eastern China: remote forcing from the two types of El Niño. J Clim 27:8778–8792

Li G, Xie SP, Du Y (2016a) Effects of excessive equatorial cold tongue bias on the projections of tropical Pacific climate change. Part I: the mean warming pattern in CMIP5 multi-model ensemble. Clim Dyn 47:3817–3831

Li XC, Xie SP, Gille ST, Yoo C (2016b) Atlantic-induced pan-tropical climate change over the past three decades. Nat Clim Chang 6:275–279

Li G, Xie SP, He C, Chen Z (2017a) Western Pacific emergent constraint lowers projected increase in Indian summer monsoon rainfall. Nat Clim Change 7:708–712

Li T, Wang B, Wu B et al (2017b) Theories on formation of an anomalous anticyclone in western North Pacific during El Niño: a review. J Meteorol Res 31:987–1006

Li G, Jian YT, Yang S et al (2019) Effect of excessive equatorial Pacific cold tongue bias on the El Niño-Northwest Pacific summer monsoon relationship in CMIP5 multi-model ensemble. Clim Dyn 52:6195–6212

Li G, Gao CJ, Lu B, Chen HS (2021a) Inter-annual variability of spring precipitation over the Indo-China Peninsula and its asymmetric relationship with El Niño-South Oscillation. Clim Dyn 56:2651–2665

Li G, Gao CJ, Xu B et al (2021b) Strengthening influence of El Niño on the following spring precipitation over the Indochina Peninsula. J Clim 34:5971–5984

Li RKK, Tam CY, Lau NC (2021c) Effect of ENSO diversity and cold tongue bias on seasonal prediction of South China late spring rainfall. Clim Dyn 57:577–591

Liu BQ, Yan YH, Zhu CW et al (2020) Record-breaking Meiyu rainfall around the Yangtze river in 2020 regulated by the sub-seasonal phase transition of the North Atlantic Oscillation. Geophys Res Lett 47:e2020GL090342. https://doi.org/10.1029/2020GL090342

Liu BQ, Zhu Cw, Jiang N, Guo L (2021) Seasonal evolution of anomalous rainband over East China regulated by sea surface temperature anomalies in the northern Hemisphere. J Clim 34:3087–3102

McGregor S, Timmermann A, Stuecker MF et al (2014) Recent walker circulation strengthening and pacific cooling amplified by Atlantic warming. Nat Clim Chang 4:888–892

Newman M, Sardeshmukh PD (2017) Are we near the predictability limit of tropical Indo-Pacific sea surface temperatures? Geophys Res Lett 44:8520–8529

Pascolini-Campbell M, Zanchettin D, Bothe O et al (2015) Toward a record of central Pacific El Niño events since 1880. Theor Appl Climatol 119:379–389

Petrova D, Koopman SJ, Ballester J, Rodó X (2017) Improving the long-lead predictability of El Niño using a novel forecasting scheme based on a dynamic components model. Clim Dyn 48:1249–1276

Qiao S, Chen D, Wang B et al (2021) The longest 2020 Meiyu season over the past 60 years: subseasonal perspective and its predictions. Geophys Res Lett 48:e2021GL093596. https://doi.org/10.1029/2021GL093596

Rayner NA, Brohan P, Parker DE et al (2006) Improved analysis of changes and uncertainties in sea surface temperature measured in situ since the mid-nineteenth century: the HadSST2 dataset. J Clim 19:446–469

Ren GY, Wu H, Chen ZH (2013) Spatial patterns of change trend in rainfall of China (in Chinese). Q J Appl Meteorol 11:322–330

Sampe T, Xie SP (2010) Large-scale dynamics of the Meiyu-Baiu rainband: environmental forcing by the westerly jet. J Clim 23:113–134

Stuecker MF, Timmermann A, Jin FF et al (2013) A combination mode dynamics of the annual cycle and the El Niño/Southern Oscillation. Nat Geosci 6:540–544

Stuecker MF, Jin FF, Timmermann A, McGregor S (2015) Combination mode dynamics of the anomalous Northwest Pacific anticyclone. J Clim 28:1093–1111

Su T, Xue F (2010) The intraseasonal variation of summer monsoon circulation and rainfall in East Asia (in Chinese). Chin J Atmos Sci 34:611–628

Sun J, Xu Y, Chen ZH, Wang K (2010) Characteristics of precipitation in central region of China over 45 years (in Chinese). Resour Environ Yangtze Basin 19:45–51

Tozuka T, Yamagata T (2003) Annual ENSO. J Phys Oceanogr 33:1564–1578

Wang CZ (2002a) Atmospheric circulation cells associated with the El Niño-Southern Oscillation. J Clim 15:399–419

Wang CZ (2002b) Atlantic climate variability and its associated atmospheric circulation cells. J Clim 15:1516–1536

Wang CZ (2019) Three-ocean interactions and climate variability: a review and perspective. Clim Dyn 53:5119–5136

Wang B, Wu R, Fu X (2000) Pacific-East Asian teleconnection: how does ENSO affect East Asian. climate? J Clim 13:1517–1536

Wang B, Wu R, Li T (2003) Atmosphere-warm Ocean interaction and its impacts on the Asian-Australian monsoon variation. J Clim 16:1195–1211

Wang B, Xiang BQ, Lee JY (2013) Subtropical high predictability establishes a promising way for monsoon and tropical storm predictions. Proc Natl Acad Sci 110:2718–2722

Wang B, Li J, He Q (2017) Variable and robust East Asian Monsoon rainfall response to El Niño over the past 60 years (1957-2016). Adv Atmos Sci 34:1235–1248

Wang JX, Zhu XF, Liu XF, Pan YZ (2018) Research on agriculture drought monitoring method of Henan Province with multi-sources data (in Chinese). Remote Sensing for Land and Resources 30:180–186

Wang P, Tam CY, Xu K (2019) El Niño-East Asian monsoon tel-econnection and its diversity in CMIP5 models. Clim Dyn 53:6417–6435

Wang P, Tam CY, Lau NC, Xu K (2021) Future impacts of two types of El Niño on East Asian rainfall based on CMIP5 model projections. Clim Dyn 56:899–916

Wen N, Liu ZY, Li T (2019) Direct ENSO impact on East Asian summer precipitation in the developing summer. Clim Dyn 52:6799–6815

Wen N, Li L, Luo JJ (2020) Direct impacts of different types of El Niño in developing summer on East Asian precipitation. Clim Dyn 55:1087–1104

Weng HY, Ashok K, Behera SK et al (2007) Impacts of recent El Niño Modoki on dry/wet conditions in the Pacific rim during boreal summer. Clim Dyn 29:113–129

Weng HY, Wu GX, Liu YM et al (2011) Anomalous summer climate in China influenced by the tropical Indo-Pacific Oceans. Clim Dyn 36:769–782

Wu R, Hu ZZ, Kirtman BP (2003) Evolution of ENSO-related rainfall anomalies in East Asia. J Clim 16:3742–3758

Wu B, Zhou TJ, Li T (2009) Seasonally evolving dominant interannual variability modes of East Asian climate. J Clim 22:2992–3005

Wu R, Yang S, Liu S et al (2010) Changes in the relationship between Northeast China summer temperature and ENSO. J Geophys Res 115:D21107. https://doi.org/10.1029/2010JD014422

Wu MN, Zhou TJ, Chen XL, Wu B (2020) Intermodel uncertainty in the projection of the anomalous western North Pacific

anticyclone associated with El Niño under global warming. Geophys Res Lett 47:e2019GL086139. https://doi.org/10.1029/2019GL086139

Wu XB, Li G, Jiang WP et al (2021) Asymmetric relationship between ENSO and the tropical Indian Ocean summer SST anomalies. J Clim 34:5955–5969

Xie SP, Zhou ZQ (2017) Seasonal modulations of El Niño-related atmospheric variability: Indo-Pacific Ocean feedback. J Clim 30:3461–3472

Xie SP, Annamalai H, Schott F, McCreary JP (2002) Structure and mechanisms of south Indian Ocean climate variability. J Clim 15:864–878

Xie SP, Hu K, Hafner J et al (2009) Indian Ocean capacitor effect on Indo-western Pacific climate during the summer following El Niño. J Clim 22:730–747

Xie SP, Du Y, Huang G et al (2010) Decadal shift in El Niño influences on Indo-western Pacific and East Asian climate in the late 1970s. J Clim 23:3352–3368

Xie SP, Kosaka Y, Du Y et al (2016) Indo-western Pacific Ocean capacitor and coherent climate anomalies in post-ENSO summer: a review. Adv Atmos Sci 33:411–432

Xue F, Liu CZ (2008) The influence of moderate ENSO on summer rainfall in eastern China and its comparison with strong ENSO. Chin Sci Bull 53:602–609

Yang JL, Liu QY, Xie SP et al (2007) Impact of Indian Ocean SST basin mode on the Asian summer monsoon. Geophys Res Lett 34:L02708. https://doi.org/10.1029/2006GL028571

Yeh SW, Kug JS, Dewitte B et al (2009) El Niño in a changing climate. Nature 461:511–514

Yong L, Huang RH (2019) Linkages between the South and East Asian monsoon water vapor transport during boreal summer. J Clim 32:4509–4524

Yu T, Feng J, Chen W (2020) Evaluation of CMIP5 models in simulating the respective impacts of East Asian winter monsoon and ENSO on the western North Pacific anomalous anticyclone. Int J Climatol 40:805–821

Yuan Y, Yang S (2012) Impacts of different types of El Niño on the East Asian climate: focus on ENSO cycles. J Clim 25:7702–7722

Yuan Y, Yang S, Zhang ZQ (2012) Different evolutions of the Philippine sea anticyclone between the eastern and central Pacific El Niño: possible effects of Indian Ocean SST. J Clim 25:7867–7883

Zhang R, Sumi A (1999) A diagnostic study of the impact of El Niño on the precipitation in China. Adv Atmos Sci 16:229–241

Zheng J, Wang C (2021) Influences of three oceans on record-breaking rainfall over the Yangtze river valley in June 2020. Sci China Earth Sci. https://doi.org/10.1007/s11430-020-9758-9

Zhou Y, Deng G, Chen H, Chen Z (2005) Synoptic features of the second Meiyu period in 1998 over China. J Meteorol Res 19:31–43

Zhou XY, Liu F, Wang B et al (2019) Different responses of East Asian summer rainfall to El Niño decays. Clim Dyn 53:1497–1515

Zhou ZQ, Xie SP, Zhang RH (2021) Historic Yangtze flooding of 2020 tied to extreme Indian Ocean conditions. Proc Natl Acad Sci 118:2022255118. https://doi.org/10.1073/pnas.2022255118

Zou Y, Yu JY, Lee T et al (2014) CMIP5 model simulations of the impacts of the two types of El Niño on the U.S. winter temperature. J Geophys Res 119:3076–3092